SAE INTERNATIONAL

2017-01-0713

Published 03/28/2017

Development of the Combustion System for Volvo Cars Euro6d VEA Diesel Engine

Håkan Persson, Aristotelis Babajimopoulos, Arjan Helmantel, Fredrik Holst, and Elin Stenmark

Volvo Car Corporation

CITATION: Persson, H., Babajimopoulos, A., Helmantel, A., Holst, F. et al., "Development of the Combustion System for Volvo Cars Euro6d VEA Diesel Engine," SAE Technical Paper 2017-01-0713, 2017, doi:10.4271/2017-01-0713.

Abstract

The demands for a future diesel engine in terms of emission compliance, CO2 emissions, performance and cost effectiveness set new requirements for the development process of the combustion system.

This paper focuses on the development of the next generation Volvo Cars diesel combustion system, which should comply with Euro 6d including Real Driving Emissions (RDE), with emphasis on the novel methods applied throughout the process.

The foundation of a high performing combustion system is formed by first determining the requirements for the system, after which the key factors that affect system performance are selected, such as the charge motion, combustion chamber geometry and injector nozzle geometry.

Based on the requirements, a robust charge motion with desired flow characteristics is defined. A new automated CFD optimization process for combustion chamber geometry and spray target is developed. From the generated Pareto front of optimal designs, the best hardware solutions are selected based on targeted attributes. An increase in knowledge is also gained by looking into the details of the simulation results for these candidates. The selected solutions are then verified by creating rapid prototype pistons for evaluation.

The development of a highly automated test scheme makes it possible to collect large amounts of test data, which allows for models to be build based on the physical testing. Using these models enables the possibility for high modularity as well as doing sensitivity studies. It is possible to reduce the number of development loops when creating combustion system variants for different requirements. The result is a robust modular combustion system that has significant improvement in efficiency in combination with a new injection strategy.

Introduction

The emission legislation for light duty diesels is continuously tightened. In parallel, OEM fleet average fuel consumption requirements are put in place with requirements on fleet average below 95g CO2/km in 2021 for Europe. A path for a continuous further reduction is also defined. In Europe the Euro 6c emission legislation will be replaced by the intermediate Euro 6d-Temp and then Euro 6d. Simultaneously the NEDC test cycle is replaced by the World Light Test Procedure (WLTP) with Real Driving Emissions (RDE) requirements additional to the test cycle. CO2 emissions are also to be established from the new WLTP with firmer rules and a more detailed CO2 break down for each vehicle variant.

The share of passenger cars in Western Europe running on diesel is above 50% [1] and has been so for a number of years. The market share for diesel in larger vehicle classes (D, E and M) is even higher. Hence, diesel engines complying with the upcoming emission legislations including RDE are an important contribution for reaching future targets for reduced CO2 emissions.

Decomposing from the vehicle, to the engine and further down to the combustion system level, meeting the legislation requirements comes down to the balance between indicated efficiency, engine out nitrogen oxides (NOx) and particulate matter, both in terms of mass (PM) and number (PN). Since Euro 4, the engines are generally equipped with a diesel particulate filter (DPF). This means that tailpipe smoke is not an issue, neither in terms of mass nor in particulate numbers. However, this is not the case for engine out (EO) smoke. High EO smoke levels mean shorter intervals between DPF regeneration as well as risk for increased wear and aging of components. At lower loads, the DPF regeneration needs to be aided by elevated temperature, meaning wasting fuel energy solely to provide heat to the catalyst without producing work on the piston.

Reducing EO NOx to approximately Euro5 tailpipe levels usually results in increased fuel consumption and thus CO2 emissions. NOx is typically suppressed by reducing flame temperature and oxygen concentration, e.g. by retarding combustion phasing and increasing

exhaust gas recirculation (EGR). Retarding combustion phasing means that the major part of the fuel is burnt later and at a lower temperature due to the expansion, which reduces NOx formation but also the effective expansion ratio and consequently thermodynamic efficiency. The benefit of this strategy is that it is normally followed by a reduction in combustion noise, related to the maximum pressure rise rate per crank angle degree (dP/dCAD). By increasing the EGR rate, fresh charge is replaced by burnt gases and the reduced oxygen concentration directly reduces flame temperature. The reduced oxygen concentration and temperature have the additional effect of decreasing the reaction rate, i.e. for a given combustion phasing the end of combustion is delayed.

Two competing processes are then in effect. The reduced flame temperature can reduce heat transfer due to a lower temperature gradient from the bulk gas to the combustion chamber walls, thus improving thermal efficiency. On the other hand, the increased burn duration may sustain high gas temperature for a longer part of the cycle and also reduce the effective expansion ratio, both of which have a negative impact on efficiency. Additionally a higher EGR rate reduces the ratio of specific heats (Cp/Cv)[2] which further reduces efficiency. Further developing an existing diesel combustion system complying with Euro 6b towards Euro 6d with balanced emissions and efficiency attributes requires a systematic approach with clear target requirements. The benefits of an efficient development process based on statistical methods was shown by Andersson et al. for the development of the Volvo Euro5 diesel engine [3]. Here the combustion chamber shapes were derived iteratively from CFD findings based on the accumulated knowledge. Design of experiments (DoE) was used in the verification stage, both for optimizing parameters, but also for analysing the sensitivity of different solutions and selecting the most robust one. Another approach is to let the CFD calculations drive the geometry changes of the combustion chamber, either in the form of DoE:s and then metamodeling of the results or in the form of a direct optimization. One direct optimization approach is described by Ge et al. [4], where geometrical parameters are set in the first stage and controllable parameters in the second step.

This paper describes the development of the new combustion system for the Volvo Cars 2-litre diesel engine family, which is intended to meet the upcoming Euro 6d requirements. The first part of the paper addresses the requirements for the combustion system, which are then used as inputs and limitations in the subsequent work. Next, emphasis is given on the novel development process used to define the combustion system layout, i.e. the combustion chamber geometry and spray targeting. Finally, the verification process is described, including the optimization of the operating conditions and also comparison with CFD results.

Requirements

To determine the best approach for the development of a new diesel combustion system both the current status and the new requirements are of importance. Even if the development is targeting a completely new engine, the current system is still a valuable reference. Knowing the capabilities and limitations of that system is the foundation for the new development.

The requirements on vehicle level need to be broken down to engine level and further converted to the absolute requirements for the combustion system. This means, for example, going from the vehicle fuel consumption in g CO_2/km for WLTC to indicated specific fuel consumption (ISFC).

The combustion system performance is evaluated at a number of steady-state operating points selected as to cover most of the important conditions that the engine will see during normal operation. The flow structure and losses in the ports are of high interest, but, otherwise, the transient behaviour of the complete engine can be decoupled from the combustion system development. The transient behaviour of the engine can simply be treated as a modified stationary load point in terms of charge quality, once the valves are closed.

Going from the vehicle-level emission legislation to EO NOx specific emissions target includes a number of steps, most important being:

- Balancing EO emissions versus exhaust aftertreatment system (EATS) efficiency in general, but also balancing for different operating conditions.
- Defining engine and EATS warm up strategy, e.g. EO cold emissions.
- Accounting for the transient behaviour of the engine during the test cycle (WLTP) and for real driving emissions (RDE).

To simplify the definition of the requirements at the combustion system level, the requirements are expressed with respect to the reference. The reference, in this case, is the combustion system developed for the VED4 Euro 6b engine that went in production at the end of 2013. The main attributes are the following:

- Specific Emissions, especially NOx/Smoke
- Fuel Consumption, ISFC
- Cost
- Performance, capability @ rated power
- Combustion Noise
- Quality/Robustness

The reference attributes compared with requirements for the new combustion system targeting Euro 6d are illustrated in Figure 1.

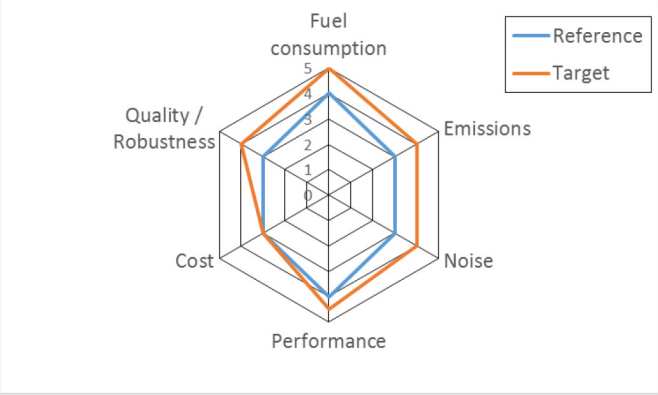

Figure 1. Combustion system requirement balance

Low engine out NOx levels are desirable, in order to reduce UREA consumption. This can be achieved with moderate EGR levels that significantly reduce EO NOx but do not cause high smoke levels. By increasing the EGR rate at higher loads, the requirements can be slightly relaxed at the lower loads, so as to avoid the need to suppress NOx to the point that fuel consumption is suffering (Figure 2).

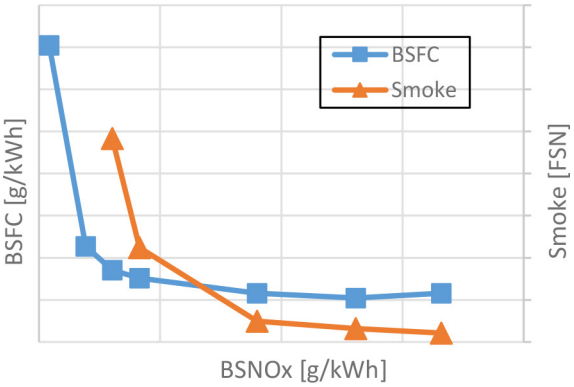

Figure 2. NOx-Efficiency trade-off and effect on smoke.

Balancing the emissions trade-off at an early stage opens up the opportunity to further address ISFC as well as performance requirements simultaneously. For example, one goal in the development work was set to reduce wall heat transfer by reducing the charge motion. By doing so, the gas exchange efficiency could also be improved by trading swirl ratio for improved port flow coefficients, the latter being a significant improvement for rated power. By reducing the charge motion, i.e. the swirling motion, the wall heat losses can be reduced [5]. However, lower heat losses do not necessarily result in increased efficiency as shown by Fridriksson et al.in [6]. The swirling motion typically interacts with the in-bowl motion after the end of injection at part load, helping to speed up the mixing-controlled combustion as described in [3]. So, the reduced swirl ratio should not increase the burn duration by slowing down the late cycle oxidation to the point that it counteracts the benefit from the reduced heat transfer.

In addition to fulfilling the CO_2 and emission requirements the system needs to be robust to component tolerances and process deviations in the production line. Tolerance chain outcome studies performed in previous internal black belt projects have led to an increased attention in certain areas. One outcome is that robustness has become an integral part of the evaluation process. The tolerance of the included angle of the injector has been shown to be the most important single factor to emission deviations. The verification process therefore includes the capability of analysing sensitivity to various parameters as shown in the test methodology chapter.

Another important contribution to improved robustness is found in the way the charge motion is created. Previously, the swirling motion was generated fully due to the port shape and was therefore highly dependent on casting tolerances. The swirl motion created by the new port designs relies to a large extent on a machined chamfer in the seat area. With this method, the desired swirl level can be created with a higher accuracy with the added benefit that the trade-off between swirl and flow capacity has improved. This, in combination with the intent to lower the swirl level, reduces the pressure losses in the intake ports significantly. The result is shown in Figure 3. The new medium performance (MP) and high performance (HP) ports show a reduced flow and increased swirl generation from the machined masking at low valve lifts, whereas a significant flow increase is achieved at higher valve lifts with reduced impact on the swirling motion.

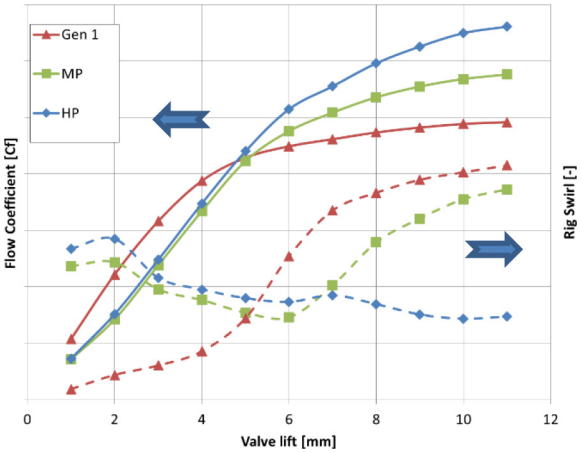

Figure 3. Measured port flow coefficients and rig swirl.

Improving each attribute without increasing cost is a clear challenge. Cost may not be added to the high-volume derivatives if it does not add substantial value. One of the main cost drivers for the combustion system is the attributes of the fuel injection system (FIE). Since the Euro 6b engine, all variants are already equipped with a system capable of 2500 bar rail pressure with closed loop control of the injected quantity. The high pressure enables a nozzle specification with good emission/CO_2 trade-off at part load. The accuracy in injected quantities enables to further develop advanced injection strategies. This leads to an improvement in the combustion noise and fuel consumption trade-off [7, 8, 9, 10].

CFD Methodology

Early in the development process, an optimization driven design method was used to identify promising combustion chamber geometries, out of which a few would be selected for prototyping and testing. In particular, a complete CFD workflow was developed in modeFrontier [11], which was then employed to optimize the piston bowl geometry, determine the best spray umbrella angle, and select the swirl level for part-load operation.

Diesel combustion was simulated using es-ice/STAR-CD [12]. The recommended physics sub-models were selected: ECFM-CLEH for combustion with the sectional method for soot formation, RNG k-ε for turbulence and the Huh spray atomization model. For an 8-hole injector, only the closed part of the cycle was simulated on a 45° degree sector mesh. The spray and combustion models were calibrated to match experimental data at two operating points: i) 4000 rpm and approximately 320 Nm; and ii) 1500 rpm and 80 Nm. The part load point was selected to be centred in the relevant operating regime and within the range covered by testing, as described in the experimental test section of the paper.

The comparison of the model predictions for cylinder pressure and rate of heat release against the experimental data can be seen in Figure 4. It should be noted that for the part-load operating point, the

post-injection has been eliminated. This is because, soot is very sensitive to post-injection and optimizing the post-injection for each piston design was outside the scope of the CFD optimization.

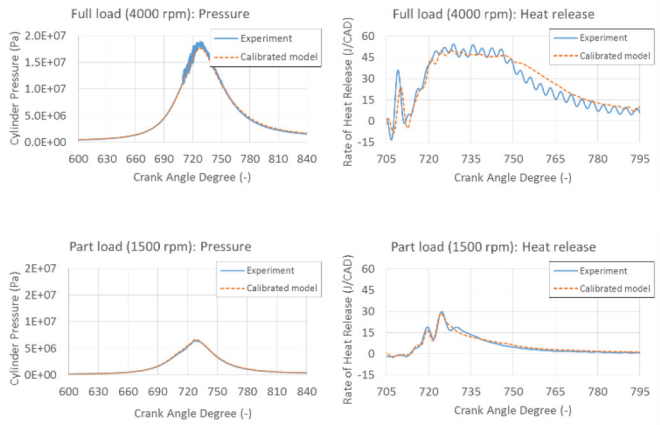

Figure 4. Model validation at full load (Upper) and part-load (Lower)

Parameterized Piston Model

In order to explore a wide range of piston bowl geometries, a fully-parameterized model was created, which describes the piston geometry with a sequence of arcs and straight segments that are connected using tangent requirements. The full piston bowl geometry, which can be seen in Figure 5, is described with a total of 12 design parameters (6 radii and 6 lengths). For each combination of values for the design parameters, the radius R4 is varied to maintain the bowl volume, and therefore the compression ratio, constant. To limit the size of the optimization problem, only 6 of the 12 design parameters were selected as independent variables in the optimization, while R4 was varied to match the target compression ratio and the rest of the parameters had fixed values. The independent parameters used in the optimization are highlighted with circles in Figure 5.

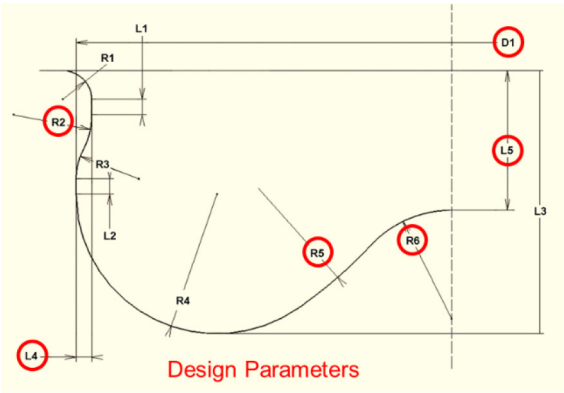

Figure 5. Schematic of piston geometry model (circled dimensions are used as independent design parameters in the optimization)

For each combination of the piston design parameters, a Matlab script was used to generate the 2-D piston profile. The profile was then used as input in STAR-CCM+ [13], which created a closed surface for the entire cylinder by generating a surface of revolution for the piston and connecting it to the liner and a simplified representation of the head surface. A 45° sector of this geometry was then meshed by es-ice and modeled by STAR-CD. The modeling workflow is shown in Figure 6.

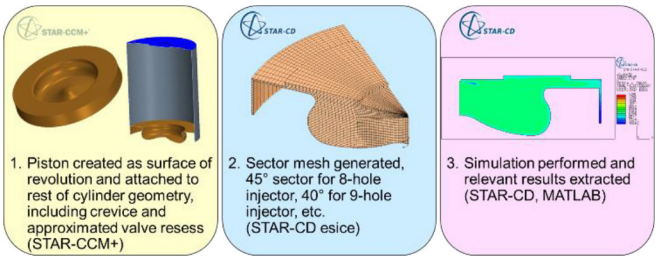

Figure 6. Diesel sector modeling workflow using STAR-CCM+ and es-ice/ STAR-CD

Optimization Workflow and Results

The complete optimization workflow was developed in modeFrontier and is shown in Figure 7. The optimization had 3 objectives:

1. Maximize full load efficiency
2. Maximize part-load efficiency
3. Minimize part-load soot

A total of 8 design variables were included. Along with the aforementioned 6 geometric design parameters, two additional design variables were used: the spray included angle and the swirl level at part load. A small pumping penalty was introduced at part load as a linear function of swirl, based on the experimentally observed increase in pumping work that was associated with higher swirl levels. For each design, a new piston geometry was computed and engine operation at full-load and part-load was simulated, using the steps described above. After the simulations finished, the results were post-processed automatically and relevant results were extracted, including efficiency values and part-load soot.

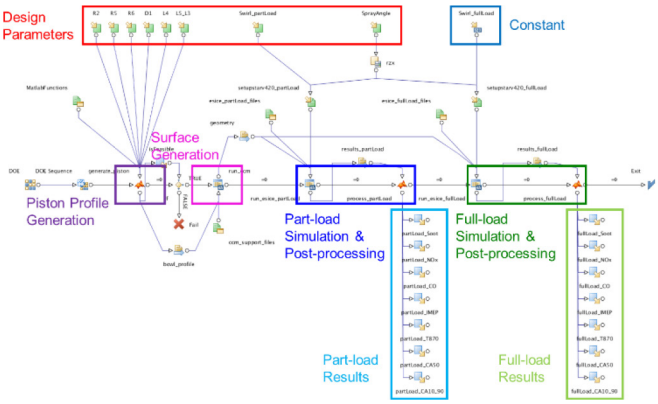

Figure 7. Optimization workflow in modeFrontier

The computational time was approximately 6 hours per operating point, so it took approximately 12 hours to fully evaluate a design. As it was possible to evaluate only 4 designs concurrently and in order to keep the total time required by the optimization under 3 weeks, modeFrontier's FAST algorithm was selected. The FAST algorithm uses response surface modeling over the regions of most interest in the design space to accelerate the optimization process. To initiate the optimization with the FAST algorithm, 55 designs were selected and evaluated using a design of experiment (DoE) based on uniform latin hypercube sampling. Subsequently, 10 generations of 10 designs each, as suggested by the FAST algoritm, were evaluated. The part-load and full-load efficiencies of the 155 simulated designs are shown in Figure 8. In the same figure, the Pareto front designs are

also highlighted. Analysis of the Pareto designs showed that part-load soot, the third design objective, was strongly correlated with part-load efficiency as seen in Figure 9, which suggested that it would be appropriate to focus only on the two efficiency objectives.

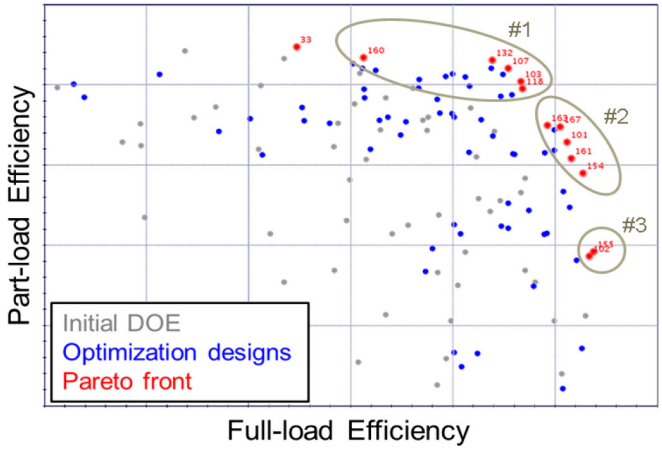

Figure 8. modeFrontier optimization results. The circles indicate Pareto designs that share geometric characteristics.

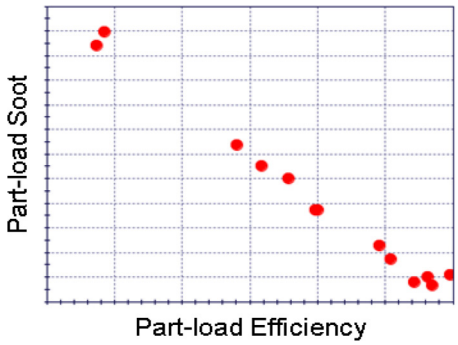

Figure 9. Part-load soot as a function of part-load efficiency

From the optimization Pareto front the top candidates were selected for verification. For this selection it was necessary to look at the detailed results as well as the individual parameter settings for each particular design. First of all, there is the direct trade-off between part load and full load efficiency along the Pareto front. The Pareto designs can be grouped into 3 distinct groups (see Figure 8) that share geometric and performance characteristics. The first group (#1) contains candidates that favour part-load efficiency, with the ones more to the right in the diagram with simultaneously improved high load efficiency. At the other end we have the designs favouring rated power efficiency (group #3). In-between, group #2 contains designs that have relatively similar high load performance with a spread in part load efficiency.

During design selection, the focus is kept primarily on the trade-off between part load and full load efficiency. As seen in Figure 9, high efficiency is strongly linked to low soot emissions, mainly due to fast combustion with good late cycle oxidation. Still there will be some deviation in smoke. The Pareto front can then be sorted to look at the calculated EO smoke levels for each design at a given balance between part load and full load efficiency.

The geometric parameter values for the designs are also of importance. The allowed range of variation is set known that there are design limitations for the piston. Two important aspects here have been the maximum bowl diameter (D1) and re-entrancy (L4). Previous studies [14] have shown improved results with a wider bowl. The wider bowls also decrease the depth of the bowl, which is an important aspect for the piston structure in withstanding high cylinder pressures and minimizing top land height. On the other hand, there needs to be sufficient space for the piston cooling gallery as well as the piston rings. L4 has shown to influence the in-bowl mixing process. One drawback with an increased L4 is that the distance between the cooling gallery and the surface of the piston lip is increased, resulting in higher surface temperatures. This can lead to overheating at rated power.

Figure 10 shows the parallel coordinates plot of the Pareto designs from Figure 8. In this plot, each design is signified by a polyline connecting vertices that lie on parallel lines, each of which corresponds to one of the design variables or optimization objectives. The length of the parallel lines represents the allowable range for each of the design variables. The polylines corresponding to the designs in the three groups marked in Figure 8 are highlighted with different colors. It is evident by the clustering of the polylines that the designs belonging to each of the groups share geometrical features:

- Group #1 designs have the largest bowl diameter (D1) and R2 radius, and are characterized by varying levels or re-entrancy (L4).
- Group #2 designs have slightly smaller D1, the largest L4, and are characterized by varying R2.
- Group #3 designs have the smallest D1 and R2 values.

From the Pareto front, three designs were selected for evaluation according to the criteria described earlier. The selected designs are marked in Figure 10 (pistons 132 and 160 from group #1 and 167 from group #2) and their shapes are shown in Figure 11. All three have high part-load efficiency, which according to Figure 9 also corresponds to lower part-load soot emissions. It can also be noted that the selected pistons have a wide span in re-entrancy (L4). The pistons performing best at full load favour large re-entrancy, which, as already discussed, is not favourable in terms of piston lip temperature.

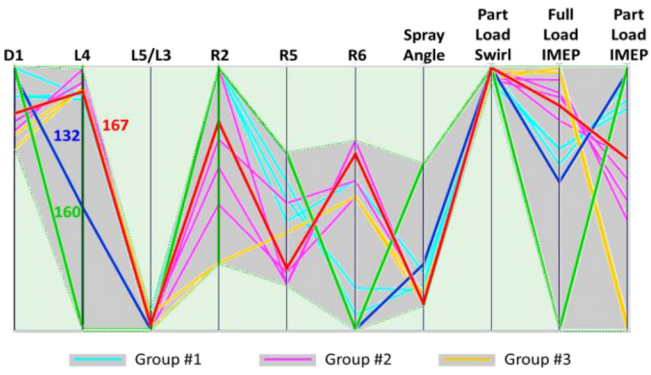

Figure 10. Parallel coordinates plot of Pareto designs. Designs are highlighted according to the grouping shown in Figure 8. Designs that were selected for evaluation are also marked.

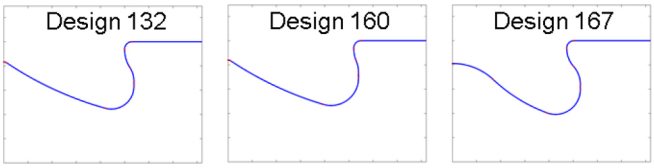

Figure 11. Geometry of Pareto designs selected for evaluation

Experimental Test Methodology

In order to verify the CFD results, the three selected piston bowl designs and a reference bowl were subjected to verification tests at both part load and maximum power. The pistons were created in-house by machining the different bowls in piston blanks, giving very short lead times.

When comparing hardware, the most important aspect is that the tests are conducted under identical conditions. However, the load/speed settings should also be both representative for the operating conditions at which the final product will spent most time in use and cover the extremities of the operating regime. At the same time, the variation in operating conditions should be limited to a manageable amount. For part load operation, three load/speed settings are presented in the paper that are both at higher and lower load and speed levels compared with the CFD part load setting (see also Figure 12). The points are specifically selected to cover low load CO and HC emissions, Soot/NOx trade-off at low lambda, and indicated efficiency with EO NOx according to requirements:

- 1280 RPM/130 Nm; constant ISNOx
- 1376 RPM/57 Nm; constant ISNOx
- 1810 RPM/107 Nm; constant ISNOx

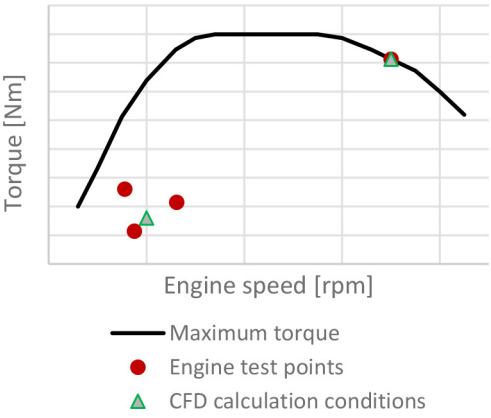

Figure 12. Engine operating conditions as a function of torque and engine speed

In addition to the part load points, maximum power was tested, while subjected to the following limits:

- $T_{exhaust,port}$: 780 °C
- p_{cyl}, max: 195 bar

During maximum power testing, the engine calibration was performed manually: boost pressure and back pressure were kept constant, while injection timing and injected fuel mass were adjusted through iteration until the above mentioned limits were met.

In order to compare the different pistons at part load under optimum conditions for each piston, a DoE test plan was set up for different part load/speed settings, using the modelling tool ASCMO by ETAS [13]. ASCMO can generate space-filling designs based on Sobol sequences which distribute factor values randomly over a chosen interval. An example of the space filling can be seen in Figure 13.

According to ETAS, Sobol sequences work best for fitting Gaussian Processes.

Besides calibration settings, different hardware combinations were also tested, some of which were part of the DoE test plan. The results where then combined in a model.

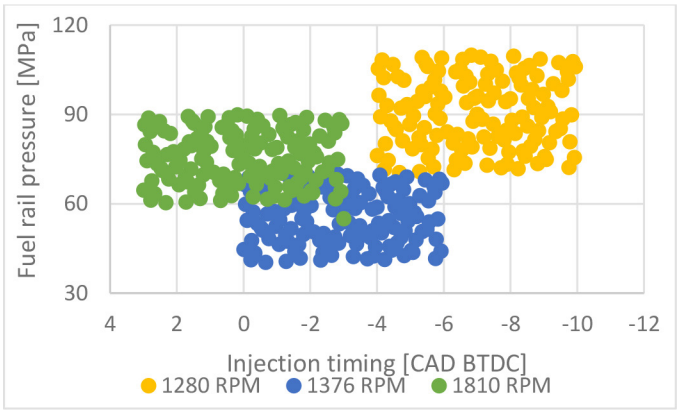

Figure 13. Example of space filling based on Sobol sequences for two factor. The same space filling is applied to all factors, of which the range is adapted to the operating point.

In order to verify the condition of the test rig, a stability check was performed each day. This checking procedure is fully automated and includes a 10 minute warm-up phase at medium load and speed, a motored test, a fired test without EGR and a repetition of the latter with the addition of EGR. The measured results are then checked and compared with previous tests, so that any drift of measuring devices or the condition of the engine or the auxiliary devices can be discovered early and rectified.

DoE Factors

The DoE factors can be divided into calibration factors (changes from test point to test point) and one hardware variable. The calibration factors included:

- Injection timing (moves the whole injection sequence back and forth)
- Swirl (swirl flap adjustment)
- Post injection mass
- Post injection interval (between main and post injections)
- Fuel rail pressure

The centre and variation span of the factors were adapted to the different load points. The tests were automated and took approximately 6-7 hours per load/speed setting (74 test points). For the pilot injections, an earlier developed strategy was used, which consists of three pilot injections, of which the 2nd and 3rd have short

intervals to the next injection. The strategy was modified for the different load points and is similar to the strategy used in the CFD simulation.

The aforementioned hardware variable is the spray target, which was adjusted by using washers of different thickness under the injector. This is a practical method that has proven to give representative results in earlier internal investigations for a limited variation in included angle. Ideally, one would like to achieve different spray targets by using nozzles with different included angles, but this would either require different injectors (each with small differences in behaviour) or the installation of different nozzles on the same injector, which would be time consuming. The spray target variation was included in the DoE test plan, meaning that the calibration variations were not simply repeated for the different washers, but that a total of 192 different combinations were split in three parts and each part was run with a different washer. That way, a greater variation of the different combinations was achieved, which enhanced model quality.

For practical reasons, the DoE test plans were simply repeated for the different pistons. For all operating points at a particular load/speed setting, the ISNOx level was kept constant by varying the EGR level. In earlier DoE test plans (for other projects), the EGR level was used as a variable, but keeping the ISNOx level constant had a number of advantages, including:

- Avoidance of test points that were too far outside the interesting ISNOx span (for example due to a combination of high fuel rail pressure, early injection timing, high swirl and low EGR)
- Avoidance of test points that resulted in excessive smoke or unstable combustion (for example due to a combination of low rail pressure, late timing, low swirl and high EGR).
- Decreased size of the DoE test plan by not having EGR as a variable.

A fixed NOx level could be used since the target requirements for EO NOx was known. This allowed the evaluation to be performed where the NOx/soot and efficiency trade-off was relevant. It would have been better to include EO NOx as a factor, allowing for the possibility to also model emission trade-off curves. However, this would have further increased the required test time and cost.

ASCMO Model

All calibration and hardware combinations served as the input for an ASCMO model, from which the performance of each piston could be determined under optimum conditions. A typical example is shown in Figure 14. The model allows for an optimized calibration for different scenarios, e.g. optimum efficiency, lowest smoke or (as in most cases) a balance of different parameters, of which the importance of the individual parameters can be individually weighted. For example, a one percent change in fuel consumption is considered more important than a one percent change in smoke emissions, so the weighting can be adjusted accordingly. Another possibility is to perform an optimization for each piston with a constraint on e.g. the maximum noise level, which will result in optimized results at the same noise level, which simplifies the comparison of the different candidates.

The calibration factors could be adapted to the individual load/speed settings, but for obvious reasons, the chosen hardware had to be the best overall compromise. For hardware variations such as, in this case the spray target, sweeps are typically made for each load level, with the hardware fixed in a number of positions and the other variables optimized for that specific case. The best compromise is then chosen after comparing the trends for the different load cases.

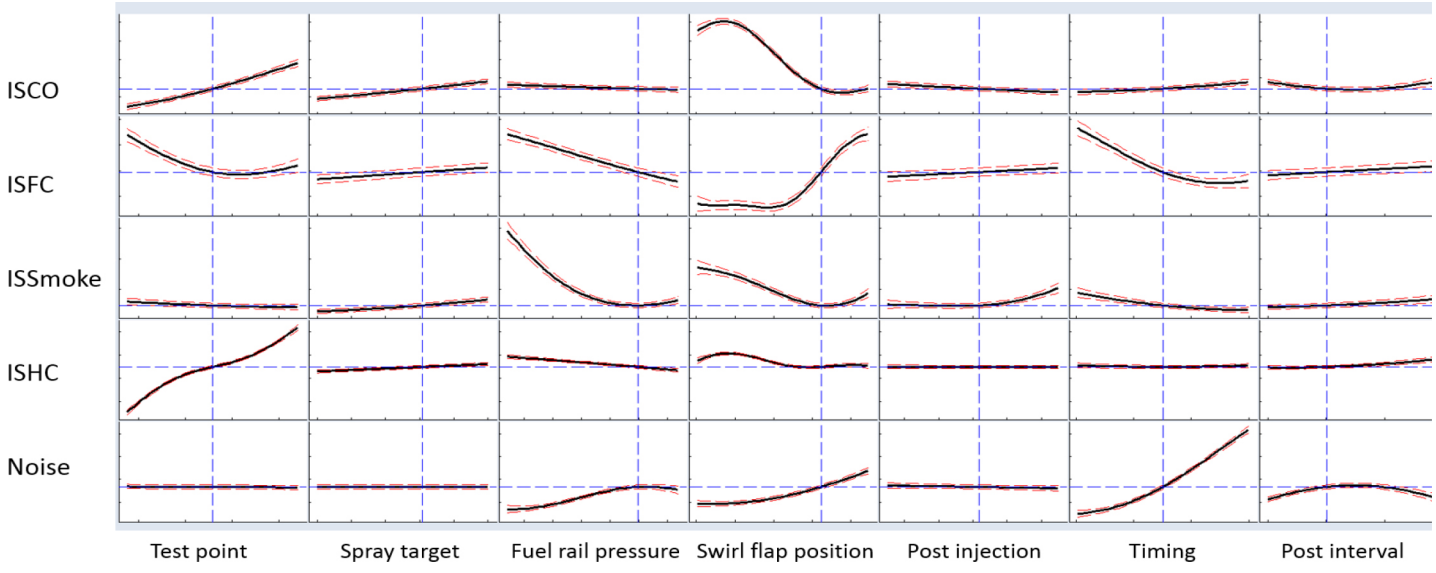

Figure 14. Example of model. Red dotted lines show standard deviation of the model.

In addition to the aforementioned calibration and hardware factors, a time factor was also included to compensate for the drift over time. Earlier testing has shown that fuel consumption drops over time and stabilizes at a lower level (~0,5-1,5%). Smoke and HC emissions are also affected. The reason for this phenomenon is likely related to the build-up of an insulating soot layer on the piston at low load operation. When the engine is operated at a fairly high load (~10 minutes at 20 bar IMEP), and the first test of the test sequence is repeated, very similar levels of fuel consumption and emissions are measured, which suggests that the soot layer is built up during low load operation and burnt off during high load operation. By including time as a variable in the model, the quality of the model was improved. The model showed that in most cases, the influence of the time factor was reduced to zero around halfway down the test points at a particular load. In order to keep the boundary conditions for each test series the same, the test program was started with the aforementioned high load point, to remove the soot from the piston.

Results

Based on DoE test results, the variables were optimized for a combination of lowest fuel consumption and smoke for a constant noise level for all pistons (engine-out NOx was kept constant for all test points within a load-speed setting). Figure 15 and Figure 16 illustrate the results for indicated fuel consumption and smoke. The absolute difference between pistons is less than what is suggested by the simulation. Piston #167 shows the worst part load efficiency of the new pistons, corresponding to the simulation results. Unfortunately, it also performs worse than the reference. Here the results are obtained with an optimized calibration for each piston, so the difference in soot as seen in the simulation results is not as pronounced.

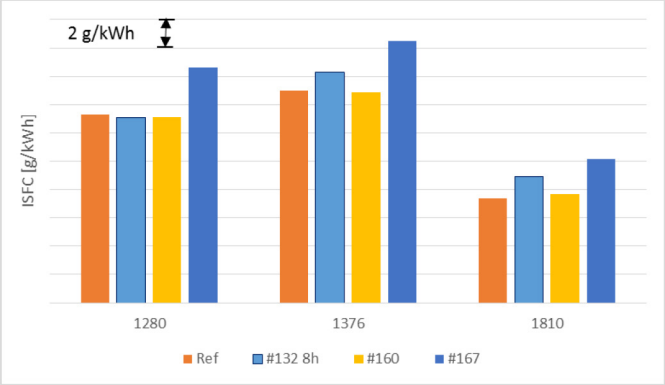

Figure 15. Indicated fuel consumption comparison at part load.

Referring back to the Requirements section, the results for the new system layout are illustrated in Figure 17. The new combustion system includes the new port concept with reduced base swirl, a new injector specification and a revised version of the close pilot injection strategy also used for the CFD optimization. Here the reference piston is still used. An improvement in ISFC of approximately 2% can be achieved with significantly reduced combustion noise in dB. This is achieved even if running with lower steady-state EO NOx levels. Only in one case there is a penalty on EO Smoke. However, the absolute level is still acceptable, and is anyway accompanied by suppressed EO NOx level.

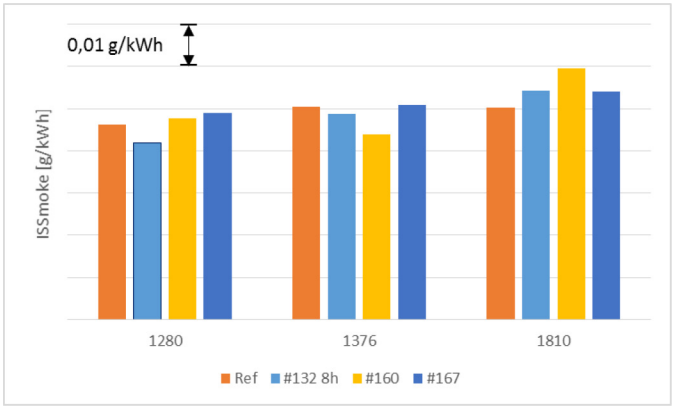

Figure 16. Indicated specific Smoke at part load.

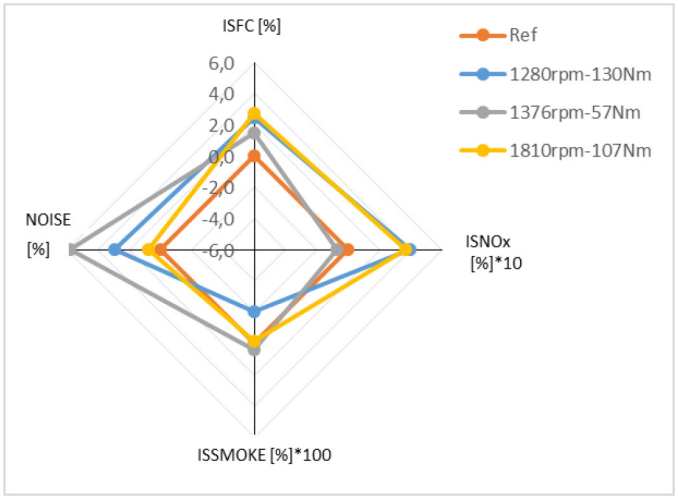

Figure 17. Improvement in ISFC, ISNOx, ISSMOKE and Noise compared to reference for part load.

Discussion

Comparing the CFD simulation results with test results needs to be done with great care for several reasons. The test results that are being compared with the CFD results are indeed an average over 3 operating points surrounding the CFD load point. This is a deliberate artefact. The alternative would be to run additional points on the engine, which was deemed too time consuming, especially since it would be very closely spaced in-between the present three points. Moreover, the CFD simulations were run with the same injection strategy for each combustion chamber and nozzle variant, whereas the test DoE included injection timing among the calibration parameters and the final test results were achieved with an optimized calibration for each piston. It is due to the fixed injection strategy that the CFD results display a larger variability in efficiency compared with the experimental data.

Figure 18 shows a comparison in efficiency for the different bowls, including the reference bowl. What can be concluded is that the part load efficiency is predicted reasonably well, but the efficiency at maximum power shows discrepancies. It should be kept in mind that that we are comparing the best designs from the CFD optimization and the absolute difference between the pistons is small according to the calculations and even smaller according to the experiments (<1%). Both the calculations and the experiments agree that pistons

132 and 160 have part-load efficiency similar to the reference piston (at least with a 159° included angle), but the reference piston performs better at maximum power than predicted.

For smoke, the results are expected to deviate, since the post injection quantity and timing is optimized for each piston and operating point in the verification test, whereas it is kept constant in the CFD optimization.

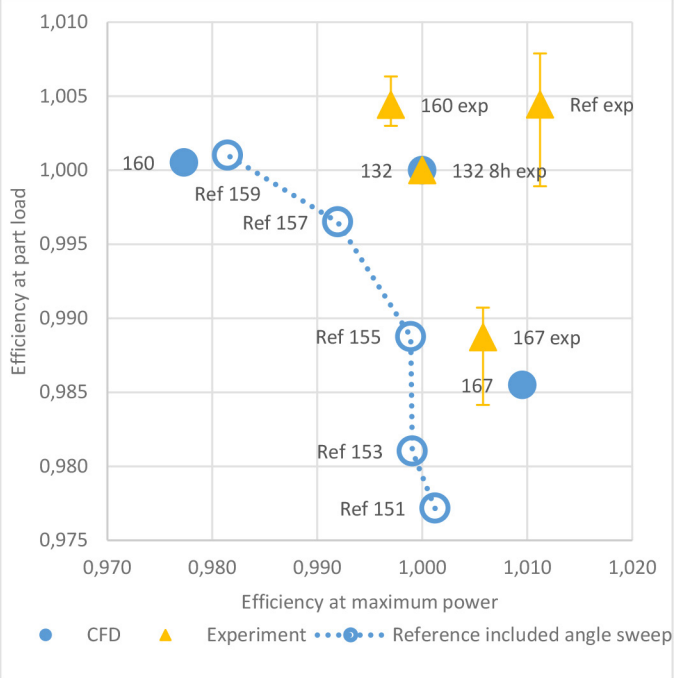

Figure 18. Comparison of CFD simulation and engine test results, relative to piston #132. Part load test results are an average, with the lines at each point indicating the range of results

Summary/Conclusions

In order to meet the Euro 6d emission regulations, a new combustions system was developed, of which the development process is described in this paper. The main contributions to the process can be summarized as follows:

- The process starts with defining clear requirements for the system, which are used as boundary conditions for the development.
- A novel simulation setup in modeFrontier, is used to drive the optimization process of the combustion chamber design and includes:

1. A parameterized model of the piston geometry and generation of piston profiles with a Matlab script.
2. Full surface generation in STAR-CCM+.
3. Meshing of the sector and simulation of part- and full-load operation with es-ice/STAR-CD.
4. Extraction of relevant results.

- An initial DoE is used to explore the design space, which includes a combination of geometrical dimensions coming from a parametrized bowl shape and physical flow and spray attributes. The direct optimization is performed using modeFrontier's FAST algorithm, which employs meta-models to accelerate the optimization process and reduce the total computational time. A number of simplifications are identified to enable the direct optimization to include both part-load and full-load.
- The resulting Pareto front of piston bowl candidates enable different properties to be selected. For example, full-load attributes can be traded for part-load fuel economy. For a given position along the Pareto front, different factors can be considered, such as swirl, maximum bowl diameter etc.
- Three of the Pareto piston designs were machined and then tested in a single cylinder engine using DoE test schemes that are set up to provide a high amount of data for the available test time. The data is then used as input for models that allow for comparing the pistons under optimized conditions for different scenarios.
- The agreement between simulation and test results was good for part load conditions but shows some discrepancy for maximum power.

References

1. ACEA, http://www.acea.be/statistics/tag/category/share-of-diesel-in-new-passenger-cars
2. Heywood, J., "Internal Combustion Engine Fundamentals",
3. Andersson, Ö., Somhorst, J., Lindgren, R., Blom, R. et al., "Development of the Euro 5 Combustion System for Volvo Cars' 2.4.I Diesel Engine," SAE Technical Paper 2009-01-1450, 2009, doi:10.4271/2009-01-1450.
4. Ge, H., Shi, Y., Reitz, R., Wickman, D. et al., "Engine Development Using Multi-dimensional CFD and Computer Optimization," SAE Technical Paper 2010-01-0360, 2010, doi:10.4271/2010-01-0360.
5. Inagaki, K., Mizuta, J., Fuyuto, T., Hashizume, T. et al., "Low Emissions and High-Efficiency Diesel Combustion Using Highly Dispersed Spray with Restricted In-Cylinder Swirl and Squish Flows," *SAE Int. J. Engines* 4(1):2065-2079, 2011, doi:10.4271/2011-01-1393.
6. Fridriksson, H., Tuner, M., Andersson, O., Sunden, B. et al., "Effect of Piston Bowl Shape and Swirl Ratio on Engine Heat Transfer in a Light-Duty Diesel Engine," SAE Technical Paper 2014-01-1141, 2014, doi:10.4271/2014-01-1141.
7. Busch, S., Zha, K., Miles P., "Investigations of closely coupled pilot and main injections as a means to reduce combustion noise in a small-bore direct injection Diesel engine", International J of Engine Research 2015, Vol. 16(1) 13-22
8. Hagen, J., Nakagawa, M., Herrmann, O., Weber, J., et al., "Diesel Combustion Potentials by Further Injector Improvement in Case of Different Engine Applications", 24th Aachen Colloquium Automobile and Engine Technology 2015
9. Schöppe, D., Atzler, F., Kastner, O., Kapphan, F., "High Performance Diesel Direct Driven Piezo Common Rail Injection System", 23rd Aachen Colloquium Automobile and Engine Technology 2014
10. Zeh, D., Hammer, J., Uhr, C., Rückle, M., "Bosch Diesel Injection Technology - Response for Every Vehicle Class", 23rd Aachen Colloquium Automobile and Engine Technology 2014
11. modeFrontier, http://www.esteco.com/modefrontier
12. STAR-CD, http://mdx.plm.automation.siemens.com/star-cd

13. STAR-CCM+, http://mdx.plm.automation.siemens.com/star-ccm-plus
14. Miles, P., Andersson, Ö., "A review of design considerations for light-duty diesel combustion systems", International J of Engine Research 2016, Vol. 17(1) 6-15
15. ETAS, http://www.etas.com/en/products/ascmo.php

Contact Information

Håkan Persson
hakan.hp.persson@volvocars.com

Definitions/Abbreviations

BSFC - Brake Specific Fuel Consumption

CF - Conformity Factor

CFD - Computational Fluid Dynamics

CO2 - Carbon dioxide

DoE - Design of Experiments

DPF - Diesel Particulate Filter

EATS - Engine After Treatment System

EGR - Exhaust Gas Recirculation

EO - Engine Out

FIE - Fuel Injection Equipment

ISFC - Indicated Specific Fuel Consumption

ISNOx - Indicated Specific Nitrogen Oxides

ISSmoke - Indicated Specific Smoke

NOx - Nitrogen Oxides

PM - Particulate Matter

PN - Particulate Number

RDE - Real driving Emissions

NEDC - New European Driving Cycle

WLTP - Worldwide harmonized Light vehicles Test Procedures

The Engineering Meetings Board has approved this paper for publication. It has successfully completed SAE's peer review process under the supervision of the session organizer. The process requires a minimum of three (3) reviews by industry experts.

ISSN 0148-7191

http://papers.sae.org/2017-01-0713